Eur Biophys J (2010) 39:1563–1571
DOI 10.1007/s00249-010-0613-z

ORIGINAL PAPER

The ionization state of D37 in *E. coli* porin OmpF and the nature of conductance fluctuations in D37 mutants

Maarten Vrouenraets · Henk Miedema

Received: 18 February 2010 / Revised: 10 May 2010 / Accepted: 12 May 2010 / Published online: 4 June 2010
© European Biophysical Societies' Association 2010

Abstract Understanding the flow of ions through *E. coli* porin outer membrane protein F (OmpF) requires knowledge of the charge state of all titratable residues located along the permeation pathway. Earlier theoretical studies proved successful in the calculation of the pK values of most residues. The (apparent) pK of Asp37 (D37), on the other hand, appeared rather sensitive to the (unknown) protein dielectric used. We addressed the protonation state of D37 experimentally by replacing D37 with a (neutral) valine. This D37V mutant expressed reduced cation selectivity, in agreement with the view that D37 in wild-type (WT) OmpF is fully ionized, i.e., deprotonated. The introduction of a (positively charged) arginine at position 37 evoked current fluctuations. Similar behavior was observed in the D37K mutant and the cysteine mutants D37C-MTSEA and D37C-MTSET. Nontitratable [2-(trimethylammonium)ethyl]-methanethiosulfonate (MTSET) carries a permanent and pH-independent charge of 1*e*, implying that the fluctuations of the D37C-MTSET mutant do not represent (de)protonation reactions of MTSET. We therefore conclude that these fluctuations reflect transitions between conformational substates evoked by structural instabilities due to the positive charge at that particular position in the pore lumen. Based on the similarities between D37C-MTSET fluctuations and those seen in the other mutants, notably D37K, the underlying mechanism of these fluctuations may be (essentially) the same in all four mutants studied.

Keywords Conductance or current fluctuations · Conformational substates · Conformation transitions · *E. coli* porin · OmpF D37 mutant · MTSET

M. Vrouenraets · H. Miedema
Biomade Technology Foundation, Nijenborgh 4,
9747 AG Groningen, The Netherlands

Present Address:
H. Miedema (✉)
Wetsus, Agora 1, 8900 CC Leeuwarden, The Netherlands
e-mail: henk.miedema@live.com

Introduction

Ion channel proteins span the membrane and create pathways for ion flow across the otherwise impermeable, low-dielectric phospholipid bilayer. The outer membrane protein F (OmpF) from *Escherichia coli* is a trimer protein consisting of three independently operating β-barrels (Schirmer 1998; Delcour 2003). Halfway down the pore these channels narrow, leaving a cross-section of approximately 0.7×1.1 nm^2 (Cowan et al. 1992). Ion permeation through channels of nanometer dimensions is dominated by electrostatics. As demonstrated by ample studies, the acid and basic amino acid residues located in this constricted zone of OmpF ("selectivity filter") clearly affect, if not dominate, the ion selectivity of the channel (Benz et al. 1978, 1979; Lou et al. 1996; Saint et al. 1996; Saxena et al. 1999; Phale et al. 2001; Bredin et al. 2002; Vrouenraets et al. 2006; Aguilella-Arzo et al. 2007; Pezeshki et al. 2009).

However, the part of the protein that forms the selectivity filter proper accounts for only a small fraction of the >100 titratable residues in a single OmpF monomer (Cowan et al. 1992; Karshikoff et al. 1994; Nestorovich et al. 2003; Alcaraz et al. 2004; Varma and Jakobsson 2004). That amino acids other than those in the constriction zone contribute to selectivity is most obvious from the observation that, although WT OmpF is cation selective,

the total, net charge of the residues that make up the constriction zone is positive. Furthermore, salt or pH gradients strongly rectify OmpF currents, an effect attributed to asymmetric distribution of permanent charge in the vestibules at either side of the constriction zone (Nestorovich et al. 2003; Alcaraz et al. 2004, 2006; Garćia-Giménez et al. 2009).

A Brownian dynamics study by Schirmer and Phale (1999) revealed cations and anions following separate routes on their way through the channel. Molecular dynamics studies by Im and Roux (2002a, b) confirmed this finding. These permeation pathways run along the entire length of the channel, implying that many more residues than those that line the selectivity filter participate in ion permeation. Im and Roux (2002a) constructed ion density maps of OmpF at different positions along the *z*-axis (i.e., perpendicular to the channel axis), using slabs of 0.4 nm thickness. In the extracellular vestibule at a distance of, on average, 1.6 nm from the selectivity filter they identified a high density of anions near (positively charged) R167 and R168. As shown in a previous study, substitution of these two arginines by two glutamates resulted in strong current rectification (Miedema et al. 2007). According to the ion density maps of Im and Roux (2002a), the highest density of cations was observed near the (negatively charged) residues E29, D37, and D74, all three located in the same plane but clearly separated from R167 and R168 (Fig. 1).

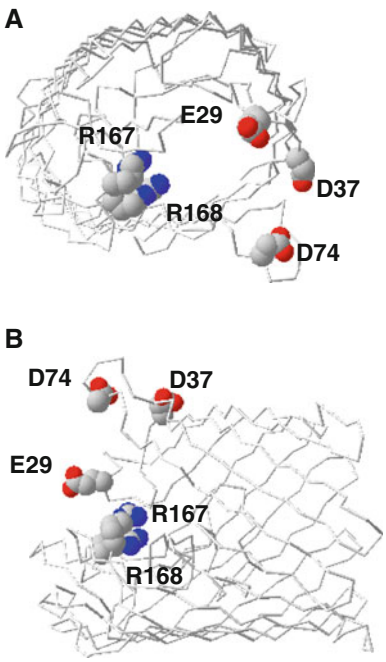

Fig. 1 Top (**a**) and side view (**b**) of a single WT OmpF monomer with the residues E29, D37, and D74 indicated. Because R167 and R168 are located in the same plane, these two residues are indicated as well (see text)

Of the three acidic residues, D37 is of particular interest because the calculation of its ionization state (pK) proved to be rather sensitive to the protein dielectric used (Varma and Jakobsson 2004). As the present study shows, the charge constellation at this point of the permeation pathway indeed clearly affects the current profile of OmpF. This is illustrated by effects on selectivity and conductance fluctuations as observed after the introduction of a positive charge at position 37. The aim of the present study is to determine the ionization state of D37 in WT OmpF and to identify the mechanism responsible for the conductance fluctuations observed in D37 mutants.

Materials and methods

The procedures for site-directed mutagenesis, OmpF isolation, and purification from inclusion bodies and details regarding electrophysiological protocols and data analysis can be found elsewhere (Miedema et al. 2004, 2006a; Vrouenraets et al. 2006). Briefly, planar lipid bilayer (PLB) experiments were performed using a Delrin cuvette (Warner Inst., Hamden, CT). Salt bridges (3 M KCl/2% agar) connected the *cis* compartment to the headstage of the Axopatch 200B amplifier (Molecular Devices Corporation, Sunnyvale, CA) and the *trans* compartment to ground. The PLB was painted across a 250-μm-diameter aperture and was composed of neutral phosphatidylcholine (PC), dissolved in *n*-decane. While stirring, ~0.2 μl 1 μg/μl OmpF stock solution in 0.1 M NaCl pH 7 buffer supplemented with 1% *n*-octyl-poly-oxyethylene detergent (OPOE; Alexis Biochemicals, San Diego, CA) was added to the *trans* side, resulting in final OPOE concentration of $\sim 5 \times 10^{-5}$%. It is generally known that detergents can evoke channel-like behavior. Control experiments, i.e., in the absence of OmpF, proved however that the membrane remained silent upon addition of OPOE at such low concentrations. Potential differences (V) are defined as $V = V_{cis} - V_{trans}$. A positive (outward) current refers to a flux of positive charge from *cis* to *trans*. Data were filtered and digitized at 1 and 5 kHz, respectively.

Ion activities were calculated using Geochem-PC 2.0 software (Parker et al. 1995). Conductance (g) was defined as the slope conductance of the fully opened trimer between ±10 mV, measured in symmetrical 0.1 M NaCl. The potential of zero current (i.e., reversal potential, E_{rev}) is a measure of the selectivity of the channel. Selectivity was assessed in a gradient of 0.1 and 1 M NaCl (0.1/1 M NaCl) as *cis*/*trans* with equilibrium potentials of Na (E_{Na}) and Cl (E_{Cl}) of −49 and 49 mV, respectively. Prior to painting the bilayer, current was zeroed using the pipette offset on the Axopatch. Therefore, measured reversal potentials (E_{rev}) have all been

corrected for a liquid junction potential of 11 mV (in 0.1/1 M NaCl). Values of E_{rev} and g were derived from current traces in response to a voltage ramp from −100 to 100 mV in ~2 s. Data analysis was performed using Clampfit 10.1 software (Molecular Devices Corporation, Sunnyvale, CA). Figure 1 was constructed using SwissPdbViewer software (version 3.7).

All chemicals including L-α-phosphatidylcholine (PC, from soybean, ≥99%) were purchased from Sigma–Aldrich. Apart from 0.1 or 1 M NaCl or KCl, recording buffers contained either 20 mM 2-(*N*-morpholino)ethanesulfonic acid (MES), 4-(2-hydroxyethyl)-1-piperazineethanesulfonic acid (HEPES) or *N*-cyclohexyl-3-aminopropanesulfonic acid (CAPS) buffer, adjusted with *n*-methyl-D-glucamine to pH 5.7, 7.4 or 10, respectively.

Chemical modification by MTS compounds

WT OmpF protein itself is cysteine free. Therefore, exposure to cysteine-dependent reagents [e.g., methanethiosulfonates (MTS)] chemically modifies only cysteines previously introduced by site-directed mutagenesis. The MTS compounds used were 2-aminoethylmethanethiosulfonate (MTSEA) and [2-(trimethylammonium)ethyl]-methanethiosulfonate (MTSET), both purchased from Anatrace, Maumee, OH. The modification efficiency can be improved by keeping the cysteines reduced (Vrouenraets et al. 2006). We therefore pretreated D37C protein with 1 mM 1,4-dithiothreitol (DTT) for 1 h. Chemical modification was achieved after overnight incubation of 5–10 μg/ml D37C protein with 50 mM MTS reagents in a 100 mM NaPi buffer, pH 7.5, containing 0.3% OPOE.

Whether or not all three monomers of a single OmpF trimer were chemically modified was assessed by studying E_{rev} recordings. Only if all three monomers are labeled and by implication have the same ion selectivity do the current traces with one, two, or three open monomers intercept the voltage axis at the same potential. Therefore, an E_{rev} value that depended on the number of open monomers was taken as proof of incomplete labeling (see Vrouenraets et al. 2006).

Folding efficiency

All mutant (and chemically modified) proteins characterized in this study formed functional trimers. From this we conclude that the mutated proteins had retained their global structural integrity (see Lou et al. 1996). Starting from inclusion bodies, there were however marked differences in protein folding efficiency. For instance, an arginine at position 74 (the D74R mutant) hardly affected the yield. In contrast, the folding efficiency of all mutants carrying the D37R mutation was relatively low.

Table 1 Summary of measured ion selectivity (E_{rev}) in 1/0.1 M NaCl solutions (with $E_{Na} = -49$ mV and $E_{Cl} = 49$ mV) and trimeric conductance (g) in 0.1 M NaCl on WT and mutant OmpF, at either pH 7.4 (A) or pH 5.7 (B)

Strain	Fluctuations	E_{rev}	g
(A) pH 7.4			
WT	No	−20.1 ± 2.6 (12)	464 ± 20 (11)
D37V	No	−11.0 ± 1.5 (10)	418 ± 11 (11)
D37R	No	(sp1) −12.8 ± 1.1 (2)	386 ± 23 (17)
	No	(sp2) −20.4 ± 1.2 (15)	
	Yes	(sp3) −27.1 ± 2.6 (10)	
D37K	No	−8.8 ± 1.8 (16)	360 ± 16 (7)
E29R	No	−12.2 ± 3.0 (11)	335 ± 20 (9)
D74R	No	−9.6 ± 1.9 (13)	357 ± 15 (17)
(B) pH 5.7			
WT	No	−19.6 ± 2.8 (16)	425 ± 15 (11)
D37V	No	−10.2 ± 2.3 (18)	378 ± 16 (11)
D37K	Yes	(sp1) −6.3 ± 1.2 (11)	342 ± 12 (12)
	Yes	(sp2) −11.9 ± 2.1 (15)	

Also indicated is whether or not fluctuations were observed. Numbers in parenthesis represent the number of independent experiments

sp1, sp2 = subpopulation 1, subpopulation 2, etc.

Results

We started out by replacing D37 with a neutral valine. When measured in 1/0.1 M NaCl, pH 7.4 solutions (with $E_{Na} = -49$ mV and $E_{Cl} = 49$ mV), the zero current or reversal potential (E_{rev}) of this D37V mutant was approximately 10 mV more positive than E_{rev} of WT (Table 1), indicating reduced cation selectivity, in accordance with the change of net charge of 1*e*. The trimeric conductance (g), recorded in symmetrical 0.1 M NaCl, was approximately 10% lower that g of WT. The next step was to substitute D37 by a (positively charged) arginine. Compared with the D37V mutant, changes due to the D37R mutation were more profound and certainly less anticipated. The D37R mutant expressed two remarkable features: first, different levels of ion selectivity and, secondly, conductance fluctuations. With all the data pooled, E_{rev} of the D37R mutant was −22.3 ± 4.6 mV. The standard deviation of 4.6 mV indicated already the rather significant variation in the data. Closer inspection of the data revealed the existence of three subpopulations. With an E_{rev} of −12.8 mV, the selectivity of only a small fraction (2 out of 27) had moved towards anion selectivity, whereas the selectivity of the majority (15 out of 27) had retained WT selectivity, as reflected by an E_{rev} of −20.4 mV. Remarkably, with an E_{rev} of −27.1 mV, more than one-third of the mutant proteins (10 out of 27) turned out to be more cation selective than WT, despite the increase of net charge of 2*e*. Although the classification into distinct subpopulations

may seem somewhat arbitrary, we think it justified. First, the differences between the subpopulations are significant statistically, and secondly, subdivision of the data reduces the standard deviation of each subpopulation to the same level as calculated for WT and for that matter all other OmpF mutant proteins studied.

The second characteristic of the D37R mutant, i.e., the presence of conductance fluctuations, was correlated to the different levels of ion selectivity observed. The current traces in Fig. 2a were recorded in asymmetrical 1/0.1 M NaCl solutions and in response to a voltage ramp protocol from −100 to 100 mV. This figure shows the two distinct current profiles most frequently observed and representative for the majority (25 out of 27) of D37R proteins studied. D37R porins with the highest cation selectivity ($E_{rev} = -27.1$ mV) all expressed current fluctuations, whereas porins expressing WT selectivity ($E_{rev} = -20.4$ mV) hardly showed this behavior. The clear link between selectivity and current profile further justifies the subdivision of D37R data into subpopulations.

Because D37 is part of the cluster of three acidic residues comprising E29, D37, and D74, we also investigated whether similar fluctuations could be evoked by introducing an arginine at positions 29 or 74. Compared with WT OmpF, the E29R and D74R mutants were approximately 10 mV less cation selective (as anticipated given the change in net charge of 2*e*) and showed >100 pS lower conductance (Table 1). However, there were no signs whatsoever of current fluctuations as observed in the D37R mutant (result not shown).

In an effort to gain more insight into the current fluctuations of the D37R mutant, we looked into the effects of ionic conditions and voltage protocol. Figure 2b shows the sensitivity of the voltage dependence of D37R fluctuations towards the ionic conditions employed. When recording in 1/0.1 M NaCl, fluctuations appeared predominantly at positive potentials. After switching to a salt gradient of 0.1/1 M NaCl, fluctuations occurred predominantly at negative potentials instead. Apparently, reversal of the polarity of the ionic gradient induces reversal of the voltage dependence of the fluctuations as well. It should be noted that the two recordings shown in Fig. 2b were obtained from a single D37R protein (after perfusion of the high-salt compartment with low-salt solution and after adding concentrated salt to the initially low-salt compartment). This means that the difference in current profile did not result from different orientation of the protein in the membrane.

Similar fluctuations as seen under asymmetrical ionic conditions were seen when recording in symmetrical 0.1 or 1 M NaCl solutions (Fig. 2c). There was, however, one main difference: the variability in behavior observed in asymmetrical solutions completely disappeared. All D37R mutants assayed showed conductance fluctuations and all

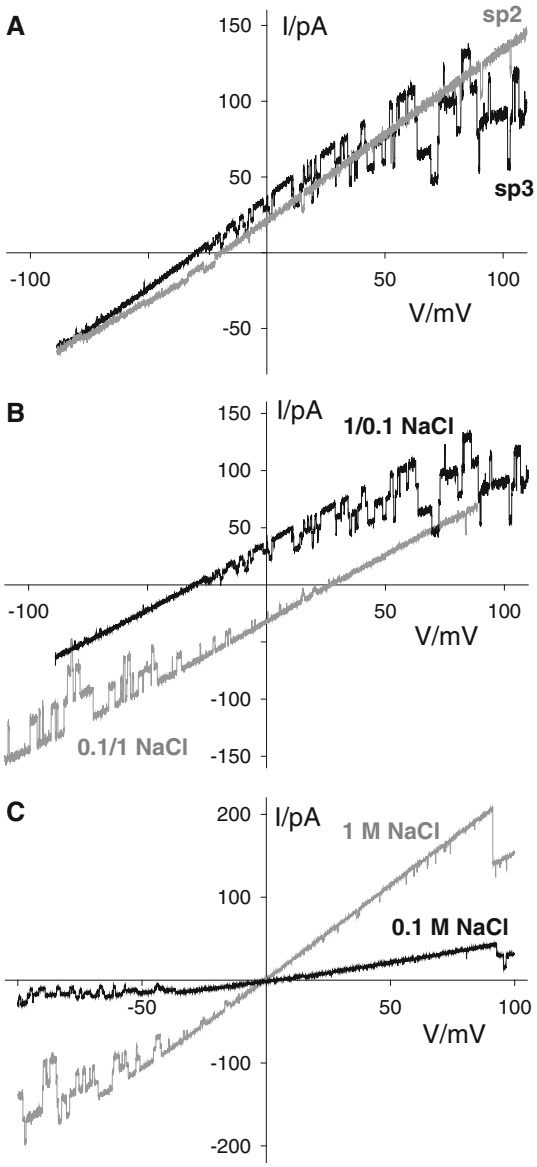

Fig. 2 **a** Current traces of the D37R mutant, recorded in asymmetrical 1/0.1 M NaCl, pH 7.4 solutions, showing the two modes of D37R behavior most frequently observed (see Table 1): sp2 (*grey*) and sp3 (*black*). Recordings were obtained from different proteins. **b** Sensitivity of the voltage dependence of the fluctuations towards the polarity of the ionic gradient employed, 1/0.1 M (*black*) or 0.1/1 M (*grey*) NaCl, pH 7.4. Recordings shown were performed on one and the same protein. **c** Recordings in symmetrical 0.1 or 1 M NaCl, pH 7.4 solutions, showing the effect of ionic strength. All recordings shown were in response to a voltage ramp protocol from −100 to 100 mV in approximately 2 s time (100 mV/s)

at negative potential only. The lack of variability in behavior under symmetrical ionic conditions is also the reason that Table 1 lists just a single conductance level for the D37R mutant.

The fluctuations of Fig. 2a were evoked by a voltage ramp protocol. Similar fluctuations could be elicited by applying a constant potential. Figure 3a shows current

traces of the D37R mutant, recorded in 1 M NaCl, pH 7.4 and with the membrane potential voltage clamped at either −100 or 100 mV. Fluctuations were observed at −100 mV only, in accordance with the response to the voltage ramp protocol shown in Fig. 2c. Note the difference in step size between the current fluctuations discussed here (lower trace) and those due to the (voltage-sensitive) gating of OmpF (upper trace). The latter typically reduce the total current magnitude by roughly one-third. Another difference between the two phenomena concerns their voltage sensitivity, i.e., the highly asymmetric voltage dependence of the D37R fluctuations versus the (almost) symmetrically, bell-shaped voltage dependence of OmpF gating. It is for these reasons that we term the transitions shown here as current fluctuations and not as gating events.

The all-point histogram belonging to a 60 min recording at −100 mV is shown in Fig. 3b. Assume that the fluctuations of a single OmpF monomer represent a two-state system. Then, the four distinct current levels observed arise from the three individual OmpF monomers that all can adopt a high (H) or low (L) conductance state with a probability to occur of p and $q = 1 - p$, respectively. The data have been fitted by Gaussians, and the numbers given refer to the fractional area (in %) under each peak, i.e., the chance to find the trimer in that particular state. Numbers in parentheses are calculated probabilities, assuming a binomial distribution. Starting with the calculation of p from the fractional surface area under one of the peaks (e.g., HHH $= p^3$), chances to find the trimer in the HLH, LHL or LLL state are $3p^2q$, $3pq^2$, and q^3, respectively (Root and MacKinnon 1994; Miedema et al. 2006b). The close resemblance between measured and theoretically expected probabilities indicates that all three monomers behave independently.

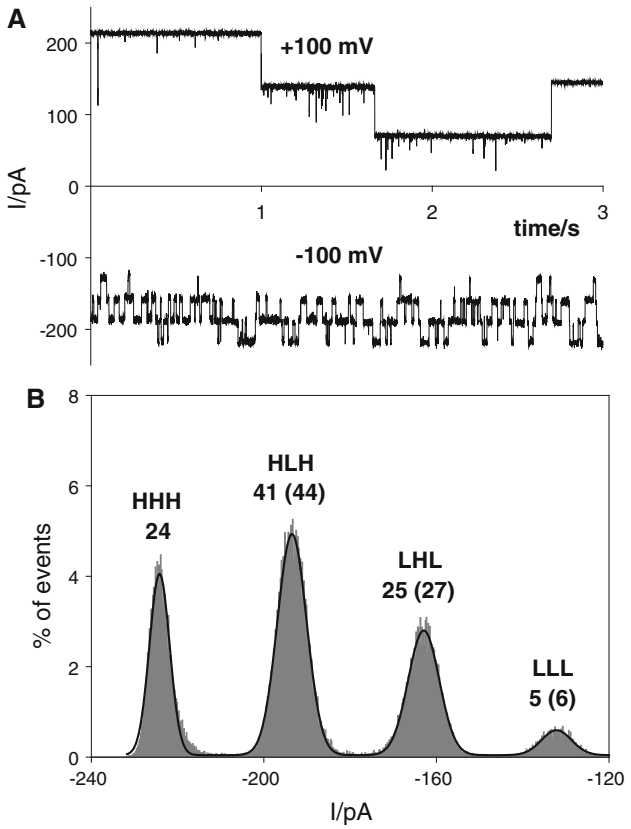

Fig. 3 **a** D37R current recordings in 1 M NaCl, pH 7.4 at either −100 or 100 mV, showing the difference in step size between the current fluctuations (at −100 mV) and voltage-sensitive gating events at 100 mV. **b** All-point histogram belonging to a 60 min recording at −100 mV. *Lines* represent fitted Gaussians and the *numbers* given refer to calculated and expected probabilities (see text). Note that the calculated probabilities add up to 95% instead of (the expected) 100%. The residual 5% is lost in between the peaks and (apparently) not accounted for by the normalized peak areas calculated by Clampfit 10.1 software

Figure 3a shows that the fluctuations of D37R are sensitive to the bias voltage applied. Although the fluctuations are sensitive to voltage, their appearance does not require a membrane potential per se as they occur in the total absence of a membrane potential as well. This is demonstrated in Fig. 4, which shows a recording of the D37R mutant obtained in 1/0.1 M KCl and with the membrane voltage clamped at 0 mV. Note that the liquid junction potential of ∼1 mV arising from the 1/0.1 M KCl gradient can safely be ignored.

The next step was to explore the specificity of the fluctuations for the presence of an arginine. We therefore replaced the arginine with either a lysine (D37K mutant) or, starting from the cysteine mutant D37C, MTSEA (the D37C-MTSEA mutant) or MTSET (the D37C-MTSET mutant). Figure 5 shows the current recordings of these D37 mutant porins and their sensitivity to pH. At pH 5.7, the D37K mutant showed similar characteristics to the D37R mutant, i.e., conductance fluctuations and different levels of ion selectivity ($E_{rev} = -6.3 \pm 1.2$ and

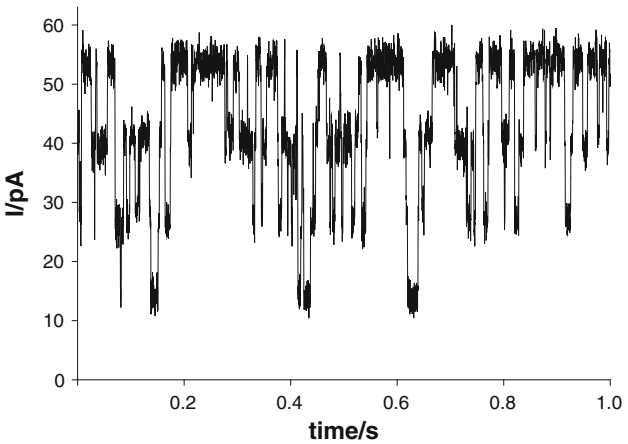

Fig. 4 Current fluctuations of the D37R mutant in 1/0.1 M KCl in the absence of an externally applied membrane potential

−11.9 ± 2.1 mV; Table 1). D37K fluctuations were effectively suppressed at pH 7.4 already. The D37R mutant, on the other hand, still demonstrated fluctuations at pH 10, though with different kinetics from those at pH 7.4. As observed with the D37K mutant, the current response of the D37C-MTSEA mutant changed gradually with pH, i.e., strong fluctuations at pH 5.7 but hardly any at pH 7.4 (data not shown) and completely silent at pH 10. D37C labeled with MTSET was the only mutant that hardly showed any pH sensitivity at all, a finding consistent with the pH-independent charge state of MTSET. Note that all four mutants showed reduced conductance at alkaline pH.

We compared the fluctuations of the D37K and D37C-MTSET mutants in a little more detail. Figure 6 shows representative all-point histograms and power spectra, both obtained from 60 s recordings at −100 mV, in symmetrical 1 M NaCl, pH 5.7 (D37K) or pH 7.4 (D37C-MTSET). As deduced from the all-point histograms in Fig. 6a, apart from a difference in distance between the peaks (i.e., conductance), chances to find the trimer in the HHH, HLH or LHL state were rather similar for the two mutant proteins. For the D37K mutant, calculated probabilities for the HHH, HLH, and LHL state are 57%, 33%, and 5%,

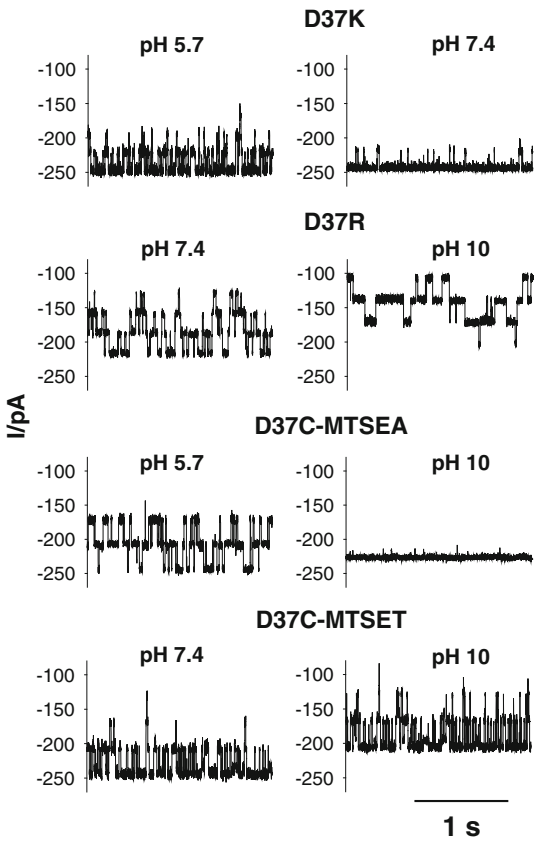

Fig. 5 pH sensitivity of the D37K, D37R, D37C-MTSEA, and D37C-MTSET mutants in 1 M NaCl and recorded at a constant potential of −100 mV. Total duration of each trace is 2 s

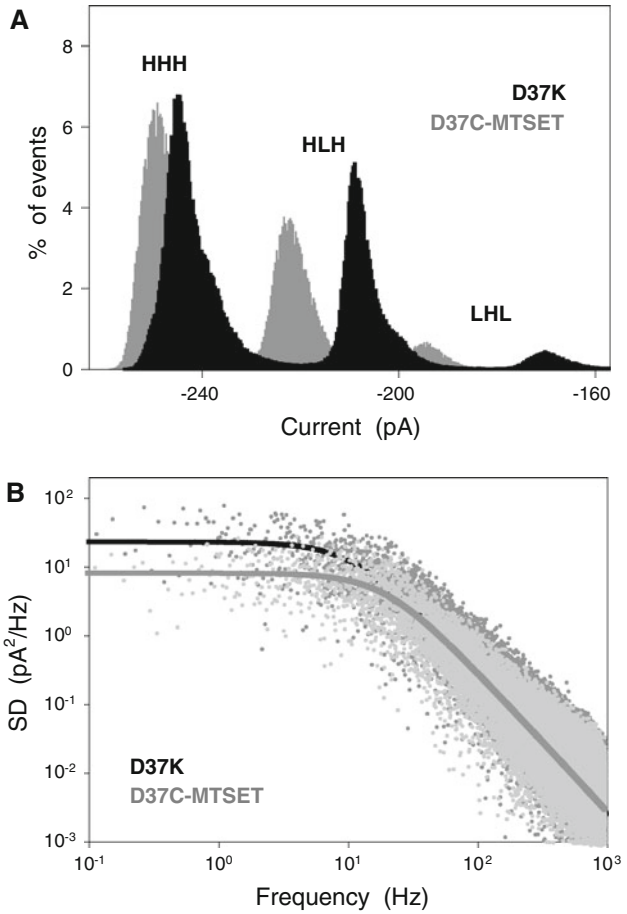

Fig. 6 **a** All-point histograms of the D37K and D37C-MTSET mutants, based on 60 s recordings at −100 mV and in 1 M NaCl, pH 5.7 (D37K) or pH 7.4 (D37C-MTSET). **b** Spectral density (SD) of D37K and D37C-MTSET. Note that both data sets largely overlap (see text). Background spectra, recorded in the absence of OmpF and at −100 mV, have been subtracted

respectively, whereas for the D37C-MTSET mutant these probabilities are 62%, 31%, and 3%. In addition, the spectral density (SD) plots of D37K (black) and D37C-MTSET (grey) largely overlapped and expressed (marginal) differences in the low-frequency domain only (Fig. 6b). The solid lines in Fig. 6b represent fits to a single Lorentzian of form $S = S(0)/[1 + (2\pi f\tau)^2]$, resulting in $S(0)$ and τ values of 24.2 pA^2/Hz and 14.8 ms for D37K and 9.4 pA^2/Hz and 8.1 ms for D37C-MTSET, respectively.

Discussion

After replacing D37 with a neutral valine, the D37V mutant lost approximately 10 mV in cation selectivity compared with WT OmpF. This finding is in accordance with the net change of charge of 2*e* and indicates that D37

in WT is fully ionized, i.e., deprotonated. The effects brought upon after the substitution of D37 by a positively charged arginine were more profound. The D37R mutant showed different selectivity levels and a current profile characterized by voltage-dependent current fluctuations, representing transitions between two conductance states. Together with residues E29 and D74, D37 has been identified as part of a cluster where cations accumulate when traversing the OmpF channel (Im and Roux 2002a). Position 37 seems unique in the sense that similar fluctuations did not occur after introduction of an arginine at either position 29 or 74 (result not shown). Residues E29 and D37 are located on loop L1, whereas D74 is part of the latching loop L2. The fact that fluctuations were seen in the D37R mutant but not in E29R indicates that there is no (clear) link between D37R behavior and its position on loop L1.

Under asymmetric ionic conditions, D37R showed different levels of ion selectivity and a corresponding current profile, i.e., either fluctuating or virtually silent (Fig. 2a). Apart from this variability, each individual D37R protein studied showed consistently one type of behavior only. Indeed, OmpF porin seems to be frozen in one particular mode of operation, as we never witnessed a protein switching from one mode to the other. This raises the question of whether the different behavior observed arises from a different orientation of D37R in the phospholipids bilayer. We think this unlikely for two reasons. Firstly, D37R is located at the inside of the (robust) β-barrel, a position that seems rather irrelevant for the way OmpF reconstitutes into the bilayer. Secondly, OmpF reconstitution shows strong preference for one particular orientation (Nestorovich et al. 2003; Alcaraz et al. 2004).

Conductance fluctuations have been described previously, for example, in the L-type calcium channel (Prod'hom et al. 1987), α-hemolysine (Kasianowicz and Bezrukov 1995), cyclic nucleotide-gated (CNG) channels (Root and MacKinnon 1994), and the nicotinic acetylcholine receptor (Danelon et al. 2007). Similar behavior has also been reported for *E. coli* porins OmpC (Liu and Delcour 1998) and OmpF (Nestorovich et al. 2003; Miedema et al. 2006b; Asandei et al. 2008). Even though the fluctuations in the present study are somehow reminiscent of the fluctuations previously observed in the D127K mutant of OmpF (Miedema et al. 2006b), there are marked differences. D37R fluctuations are strongly voltage dependent (Fig. 2a), sensitive towards the polarity of the ionic gradient employed (Fig. 2b), but insensitive towards the ionic strength of the recording solution, at least in the range 0.1–1 M (Fig. 2c). In contrast, fluctuations of the D127K mutant were observed at both negative and positive potentials and could be effectively suppressed by high-ionic-strength solutions. Some of the studies referred to above attributed observed fluctuations to protonation and deprotonation reactions of titratable residues, and others to conformational oscillations caused by structural instabilities. In the case that (de)protonation reactions are involved, Prod'hom et al. (1987) distinguished two possible scenarios, the first one based on electrostatic proton block, and the second one representing charge-induced conformational transitions. Apart from the precise underlying mechanism of fluctuations that arise from (de)protonation reactions, in both cases the frequency of fluctuations should follow the frequency of (de)protonation reactions.

The four D37 mutants characterized in the present study all introduce a chemical group of entirely different nature at position 37. Lysine (the D37K mutant) possesses a butyl ammonium side-chain with (model) pK of 10.5; arginine (the D37R mutant), a guanidine group with a pK of 12.5; MTSEA (the D37C-MTSEA mutant) is a primary amine with pK of 8.5; whereas MTSET (the D37C-MTSET mutant) is a quaternary amine that is positively charged irrespective of pH (Steidl and Yool 2001). The behavior of the D37R and D37C-MTSEA mutants seem to follow the model pK values of arginine (12.5) and MTSEA (8.5), at least for the limited pH values tested (Fig. 5). As for the D37K mutant, fluctuations occurred at pH 5.7 but not pH 7.4. Depending on the electrostatic environment, the apparent pK of an amino acid residue can deviate significantly from its model pK (Karshikoff et al. 1994; Alcaraz et al. 2004; Varma and Jakobsson 2004, 2006; Ng et al. 2008). The lack of fluctuations at pH 7.4 in D37K indicates a downshift of the pK of lysine from its model pK of 10.5 to a value <7.4. It should be noted that, from the data shown, it is not apparent whether or not the pK values of arginine and/or MTSEA were subjected to a similar downshift as well. The D37C-MTSET mutant shows sensitivity towards pH as anticipated in that it showed very similar fluctuations at pH 7.4 and pH 10, consistent with its pH-independent charge state. The fixed charge state of MTSET allows identification of the nature of the fluctuations observed in the sense that it dismisses the possibility that the fluctuations reflect (de)protonation reactions of MTSET. Apparently, the mere presence of a permanent positive charge at this particular position evokes transitions between conformational substates. Even though we recorded these transitions when applying a potential and/or ionic gradient, it is not known whether one or both conditions are actually a prerequisite for the fluctuations to occur. Obviously, the study of protein conformational switches by means of current oscillations under symmetrical experimental conditions is beyond the reach of electrophysiological techniques.

Compared with D37C-MTSET fluctuations, the nature of the fluctuations seen in the other mutants is more open to speculation. The chemical diversity of the groups introduced at position 37 may cause the underlying mechanism

of the fluctuations in the four mutants to be different as well. Even though the present study remains inconclusive on this issue, there are several arguments that nevertheless favor the view that in all four mutants essentially the same mechanism may be responsible for the fluctuations observed. Firstly, despite the entirely different nature of the chemical moiety present at position 37, all mutants demonstrated the same voltage sensitivity, i.e., at negative potential only (Fig. 5, recordings at positive potentials not shown; for comparison, see also Fig. 2a). Secondly, the all-point histograms and spectral density plots of D37K and D37C-MTSET show strong similarity (Fig. 6). Lastly, the conclusion that the fluctuations reported here reflect structural instabilities induced by a permanent charge seems to fit with the relatively low folding efficiency of D37 mutants compared with, for instance, D74R (see also Phale et al. 1998) and WT OmpF. Finally, it should be realized that, in general, pH sensitivity does not imply per se that the fluctuations themselves reflect (de)protonation reactions but instead represent conformational transitions induced by a permanently (de)protonated (chemically modified) residue.

In conclusion, the results presented herein show once more that residues other than those located in the selectivity filter proper contribute to the ion flow through the pore lumen of OmpF. At relatively large distance from the constriction zone, the charge constellation at position 37 has a marked influence on the permeation profile of the channel. This becomes most evident after replacing D37 with a positively charged arginine, lysine or one of the cysteine-bound MTS reagents. Because the D37V mutant was silent (i.e., no fluctuations), D37R behavior seems to be related to the presence of a positively charged arginine rather than to the absence of a (negatively charged) aspartate. Apart from the current fluctuations observed, another surprising finding was that more than one-third of the D37R mutant proteins assayed demonstrated improved cation selectivity, despite the change in net charge of $2e$. This study emphasizes the point that ion permeation through a nanostructure such as OmpF is a steep function of both shape and charge distribution within the pore lumen. Just a slight change in protein conformation may suffice to accomplish dramatic effects. This is even true for a robust and rather rigid β-barrel such as OmpF.

Acknowledgments This research is supported by NanoNed, a nanotechnology program from the Dutch Ministry of Economic Affairs.

References

Aguilella-Arzo M, Garćia-Celma JJ, Cervera J, Alcaraz A, Aguililla VM (2007) Electrostatic properties and macroscopic electrodiffusion in OmpF porin and mutants. Bioelectrochemistry 70:320–327

Alcaraz A, Nestorovich EM, Aguilella-Arzo M, Aguililla VM, Bezrukov SM (2004) Salting out the ionic selectivity of a wide channel: the asymmetry of OmpF. Biophys J 87:943–957

Alcaraz A, Ramírez P, Garćia-Giménez E, López ML, Andrio A, Aguilella VM (2006) A pH-tunable nanofluidic diode: electrochemical rectification in a reconstituted single ion channel. J Phys Chem B 110:21205–21209

Asandei A, Mereuta L, Luchian T (2008) Influence of membrane potentials upon reversible protonation of acidic residues from the OmpF eyelet. Biophys Chem 135:32–40

Benz R, Janko K, Boos KW, Läuger P (1978) Formation of large, ion-permeable membrane channels by the matrix protein (porin) of *Escherichia coli*. Biochim Biophys Acta 511:305–319

Benz R, Janko K, Läuger P (1979) Ionic selectivity of pores formed by the matrix protein (porin) of *Escherichia coli*. Biochim Biophys Acta 551:238–247

Bredin J, Saint N, Malléa M, Dé E, Molle G, Pagès J-M, Simonet V (2002) Alteration of pore properties of *Escherichia coli* OmpF induced by mutation of key residues in anti-loop 3 region. Biochem J 363:521–528

Cowan SW, Schirmer T, Rummel G, Steiert M, Ghosh R, Pauptit RA, Jansonius JN, Rosenbusch JP (1992) Crystal structures explain functional properties of two *E. Coli* porins. Nature 358:727–733

Danelon C, Grandl J, Hovius R, Vogel H (2007) Modulation of proton-induced current fluctuations in the human nicotinic acetylcholine receptor. Biochim Biophys Acta 1768:76–98

Delcour AH (2003) Solute uptake through general porins. Front Biosci 8:1055–1071

Garćia-Giménez E, Alcaraz A, Aguilella VM, Ramírez P (2009) Directional ion selectivity in a biological nanopore with bipolar structure. J Membrane Sci 331:137–142

Im W, Roux B (2002a) Ions and counterions in a biological channel: a molecular dynamics simulation of OmpF porin from *Escherichia coli* in an explicit membrane with 1 M KCl aqueous salt solution. J Mol Biol 319:1177–1197

Im W, Roux B (2002b) Ion permeation and selectivity of OmpF porin: a theoretical study based on molecular dynamics, Brownian dynamics, and continuum electrodiffusion theory. J Mol Biol 322:851–869

Karshikoff A, Spassov V, Cowan SW, Ladenstein R, Schirmer T (1994) Electrostatic properties of two porin channels from *Escherichia coli*. J Mol Biol 240:372–384

Kasianowicz JJ, Bezrukov SM (1995) Proton dynamics of the α-toxin ion channel from spectral analysis of pH-dependent current fluctuations. Biophys J 69:94–105

Liu N, Delcour AH (1998) The spontaneous gating activity of OmpC porin is affected by mutations of a putative hydrogen bond network or of a salt bridge between the L3 loop and the barrel. Protein Eng 11:797–802

Lou K-L, Saint N, Prilipov A, Rummel G, Benson SA, Rosenbusch JP, Schirmer T (1996) Structural and functional characterization of OmpF porin mutants selected for larger pore size. J Biol Chem 271:20669–20675

Miedema H, Meter-Arkema A, Wierenga J, Tang J, Eisenberg B, Nonner W, Hektor H, Gillespie D, Meijberg W (2004) Permation properties of an engineered bacterial OmpF porin containing the EEEE-locus of Ca^{2+} channels. Biophys J 87:3137–3147

Miedema H, Vrouenraets M, Wierenga J, Eisenberg B, Gillespie D, Meijberg W, Nonner W (2006a) Ca^{2+} selectivity of a chemically modified OmpF with reduced pore volume. Biophys J 91:4392–4400

Miedema H, Vrouenraets M, Wierenga J, Eisenberg B, Schirmer T, Baslé A, Meijberg W (2006b) Conductance and selectivity

fluctuations in D127 mutants of the bacterial porin OmpF. Eur Biophys J 36:13–22

Miedema H, Vrouenraets M, Wierenga J, Meijberg W, Robillard G, Eisenberg B (2007) A biological porin engineered into a molecular, nanofluidic diode. Nano Lett 7:2886–2891

Nestorovich EM, Rostovtseva TK, Bezrukov SM (2003) Residue ionization and ion transport through OmpF channels. Biophys J 85:3718–3729

Ng JA, Vora T, Krishnamurthy V, Chung S-H (2008) Estimating the dielectric constant of the channel protein and pore. Eur Biophys J 37:213–222

Parker DR, Norvell WA, Chaney RL (1995) GEOCHEM-PC: a chemical speciation program for IBM and compatible personal computers. In: Loeppert RH, Schwab AP, Goldberg S (eds) Chemical equilibrium and reaction models. SSSA, Special publication number 42, Soil Science Society of America/ American Society of Agronomy, Madison, WC, pp 253–269

Pezeshki S, Chimerel C, Bessonov AN, Winterhalter M, Kleinekathöfer U (2009) Understanding ion conductance on a molecular level: an all-atom modeling of the bacterial porin OmpF. Biophys J 97:1898–1906

Phale PS, Philippsen A, Kiefhaber T, Koebnik R, Phale VP, Schirmer T, Rosenbusch JP (1998) Stability of trimeric OmpF porin: the contributions of the latching loop L2. Biochemistry 37:15663–15670

Phale PS, Philippsen A, Widmer C, Pahe VP, Rosenbusch JP, Schirmer T (2001) Role of charged residues at the OmpF porin channel constriction probed by mutagenesis and simulation. Biochemistry 40:6319–6325

Prod'hom B, Pietrobon D, Hess P (1987) Direct measurement of proton transfer rates to a Group controlling the dihydropyridine-sensitive Ca^{2+} channel. Nature 329:243–246

Root MJ, MacKinnon R (1994) Two identical noninteracting sites in an ion channel revealed by proton transfer. Science 265:1852–1856

Saint N, Lou K-L, Widmer C, Luckey M, Schirmer T, Rosenbusch JP (1996) Structural and functional characterization of OmpF porin mutants selected for larger pore size. J Biol Chem 271:20676–20680

Saxena K, Drosou V, Maier E, Benz R, Ludwig B (1999) Ion selectivity reversal and induction of voltage-gating by site-directed mutations in the *Paracoccus denitrificans* porin. Biochemistry 38:2206–2212

Schirmer T (1998) General and specific porins from bacterial outer membranes. J Struct Biol 121:101–109

Schirmer T, Phale PS (1999) Brownian dynamics simulation of ion flow through porin channels. J Mol Biol 294:1159–1167

Steidl JV, Yool AJ (2001) Distinct mechanisms of Block of Kv1.5 channels by tertiary and quaternary amine clofilium compounds. Biophys J 81:2606–2613

Varma S, Jakobsson E (2004) Ionization states of residues in OmpF and mutants: Effects of dielectric constant and interactions between residues. Biophys J 86:690–704

Varma S, Jakobsson E (2006) The influence of amino acid protonation states on molecular dynamics simulations of the bacterial porin OmpF. Biophys J 90:112–123

Vrouenraets M, Wierenga J, Meijberg W, Miedema H (2006) Chemical modification of the bacterial porin OmpF: gain of selectivity by volume reduction. Biophys J 90:1202–1211